RECENT BEAM MEASUREMENTS AND NEW INSTRUMENTATION AT THE ADVANCED LIGHT SOURCE*

F. Sannibale[#1], K. Baptiste[1], W. Barry[1], M. Chin[1], D. Filippetto[2], L. Jaegerhofer[4], J. Julian[1], S. Kwiatkowski[1], R. Low[1], D. Plate[1], G. Portmann[1], D. Robin[1], T. Scarvie[1], G. Stupakov[3], J. Weber[1], M. Zolotorev[1],

[1]Lawrence Berkeley National Laboratory, Berkeley, CA 94720, U.S.A.
[2]Istituto Nazionale di Fisica Nucleare, Laboratori Nazionali di Frascati, 00044 Frascati, Italy
[3]Stanford Linear Accelerator Center, Stanford, CA 94309 U.S.A.
[4]Vienna University of Technology, 1040 Vienna, Austria

Abstract

The Advanced Light Source (ALS) in Berkeley was the first of the soft x-ray third generation light source ever built, and since 1993 has been in continuous and successful operation serving a large community of users in the VUV and soft x-ray community. During these years the storage ring underwent through several important upgrades that allowed maintaining the performance of this veteran facility at the forefront. The ALS beam diagnostics and instrumentation have followed a similar path of innovation and upgrade and nowadays include most of the modern and last generation devices and technologies that are commercially available and used in the recently constructed third generation light sources. In this paper we will not focus on such already widely known systems, but we will concentrate our effort in the description of some measurements techniques, instrumentation and diagnostic systems specifically developed at the ALS and used during the last few years.

INTRODUCTION

The Advanced Light Source (ALS) at the Lawrence Berkeley National Laboratory (LBNL) was the first soft x-ray source built among the so-called third generation synchrotron light sources [1]. In this kind of storage rings, fully dedicated to and optimized for the production of synchrotron radiation, insertion devices in the straight sections allow for many order of magnitude increased brigthness respect to those of the previous generation light sources. After the ALS many other 3rd generation sources have been and are still being built around the world under the always increasing requests from users. Despite its age, the ALS performance as a storage ring as well as a light source compare well with those of the younger machines in the category. This is due to the fact that during these years the machine underwent to a number of upgrades of the lattice, of the ring and beamline components, and of the instrumentation and beam diagnostics systems.

In this paper, after a brief introduction of the ALS and its instrumentation, we focus on the description of three new systems developed at the ALS that improve the beam measurements capabilities and potentially allow for the operation of the ring in a new mode of operation.

THE ADVANCED LIGHT SOURCE

Figure 1 shows the "clock diagram" of the ALS with its collection of beamlines. More than 40 beamlines with source points inside dipoles or insertion devices allow for more than 2000 users per year, using photons from the far-infrared to the hard x-rays. Figure 1 also shows the injector system composed by a 50 MeV linac and by a booster ring that ramps the beam energy up to 1.9 GeV before the injection into the storage ring.

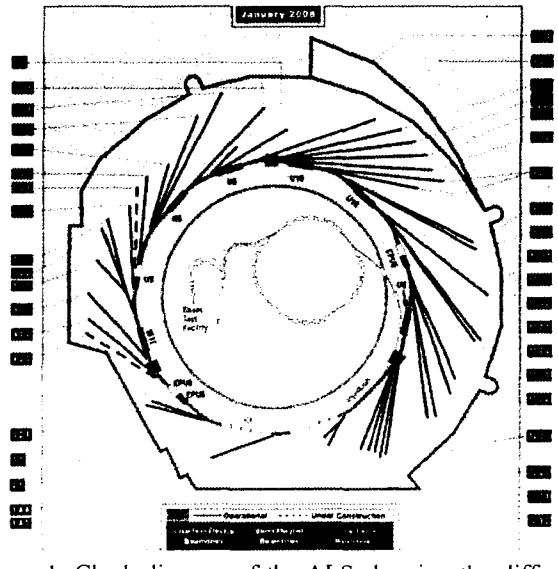

Figure 1. Clock diagram of the ALS showing the different beamlines now in operation.

* Work supported by the Director, Office of Science, of the U.S. Department of Energy under Contract DE-AC02-05CH11231.
# FSannibale@lbl.gov

Table 1 contains the main parameters of the storage ring. During standard user operation, 400 mA of electrons are stored in about 280 of the 328 available buckets. The 12 triple bend achromat cells distributed over a circumference of ~ 197 m allow for the small emittance value of 6.3 nm. A cost effective upgrade of the ALS is being proposed that will reduce the emittance by about a factor 3 by replacing four corrector magnets in each sector of the ring with the same number of hybrid elements with both dipolar and sextupolar field components [2].

Table 1: ALS ring parameters

Parameter	Value
Circumference	196.8 m
Particle Species	electrons
Beam Energy	1.9 GeV
Beam Current	400 mA
Emittance	6.3 nm
Energy Spread	0.1% rms
Radio Frequency	499.642 MHz
Harmonic Number	328
Bucket Spacing	2 ns
Lattice Cell Type	Triple bend achromat
Number of Cells	12

A CONTINUOUS EVOLUTION

Table 2 enumerates most of the beam diagnostic systems and instrumentation presently in operation at the ALS and at its injector.

Such a set is pretty complete and allows for the measurement of all the electron and photon beam relevant physical quantities and for the full control of the stability of the beam at the required level.

The majority of these individual systems have been added and/or upgraded during the years by using the latest available commercial technologies or by in house developments.

NEW INSTRUMENTATION AND BEAM DIAGNOSTICS SYSTEMS AT THE ALS

In this section we describe three in house developed systems that have been installed in the ALS in the last few years. A novel type of absolute bunch length monitor, the instrumentation that should allow running the ALS in a new operation mode defined as "pseudo-single bunch", and finally a FPGA based system that allow for the removal of undesired electrons from nominally empty buckets ("bunch cleaning").

Absolute bunch length from incoherent radiation fluctuation analysis.

Charged particles can radiate in many ways, by synchrotron radiation, Cerenkov radiation, transition radiation, etc. In all radiating processes the presence of incoherent radiation is due to the fact that the particles are randomly distributed along the beam.

For example, in the case of an ideal coasting beam composed of a large number of particles equally separated by a longitudinal distance d and moving along a circular trajectory, there is no synchrotron radiation emission apart at those wavelengths where $\lambda = nd$, with n being an integer. Additionally, for those wavelengths the radiation from different particles is in phase and the emission is fully coherent. For all other wavelenghts, the interference between the radiation emitted by the evenly distributed electrons will produce a vanishing net radiation field.

Table 2: ALS instrumentation and diagnostic systems

Monitor	Quantity
Synchrotron Light Monitors	2
Beam Position Monitors (electromagnetic, photon)	~140
DCCT's	2
Beam Loss Monitors	~24
Streak Cameras	1
Fluorescent Screens	12
Integrated Current Monitors	4
Fast Current Transformers	1
Pinger Systems	1
Slow and Fast Orbit Feedbacks	2
Bunch by Bunch Longitudinal Feedbacks	1
Bunch by Bunch Transverse Feedbacks	2
Network Analyzers	1
Real Time Spectrum Analyzers	1

In a more realistic coasting beam, the same particles are now randomly distributed along the orbit causing a small modulation of the beam distribution. The effect of such a random modulation is that the interference is not fully destructive anymore and a net nonzero radiation field shows up. If the turn by turn position of the particles along the beam changes (due for instance, to longitudinal dispersion or to path length dependence on transverse position), then

the modulation changes and the energy radiated in a single pass fluctuates turn by turn. By measuring the radiation intensity over multiple passages, we would observe that for a sufficiently large number of samples, the measured average spectrum converges to the characteristic incoherent spectrum of the radiation process under observation (synchrotron radiation in our example).

The passage from the coasting to the bunched beam case introduces a strong coherent emission at those wavelengths comparable or longer than the bunch length, but does not modify the short wavelength part of the spectrum.

It has been shown [3] for the case of a bunched beam, that by measuring the pulse to pulse intensity fluctuation of the radiation within a bandwidth $\Delta\omega$ in a region of the spectrum where no coherent emission is present, it is possible to perform absolute measurements of the bunch length. Experimental schemes exploiting such a technique and using a high resolution spectrometer have been already proved experimentally [4-6].

At the ALS, we developed a remarkably simpler version that does not require complex and expensive intrumentation and that allows for accurate absolute measurements of the rms bunch length. The scheme is non-destructive and can be applied in both circular and linear accelerators including cases where the very short length of the bunches makes difficult the use of other techniques.

The energy radiated by the bunch in a single pass is measured. The photons are collected within a narrow bandwidth in a wavelength region where no coherent emisssion is present. The values of radiated energy per passage W are measured and recorded for many passages of the beam. The method is quite general and can be applied to arbitrary bunch and bandwidth shapes. Nevertheless, in the simple but important case where both the bunch and the bandwidth shapes are Gaussian, the system equations can be integrated and an analytical solution can be derived. This case is quite realistic because commercial narrowband interferometric filters have usually a Gaussian shape and electron bunches in storage rings are usually Gaussian as well. If we use one of such filters with rms bandwidth σ_ω to measure a Gaussian beam with rms length σ_τ (measured in time units), W fluctuates passage to passage with a relative rms variation δ given by [3, 4]:

$$\delta^2 = \frac{\sigma_W^2}{\langle W \rangle^2} = 1/\sqrt{1 + 4\sigma_\tau^2 \sigma_\omega^2} \qquad (1)$$

This last expression shows that if σ_ω is known, then by measuring δ one can derive the absolute value of the rms bunch length. For nongaussian distributions the system equations need to be integrated numerically, but it can be shown that equation (1) can be still used with a few percent accuracy for most of the distributions, as long as they are represented by their rms length and do not include microstructures with characterisitc length much smaller than the bunch length.

For $\sigma_\tau >> 1/(2\sigma_\omega)$, we have that Eqn. (1) becomes $\delta^2 \sim 1/(2\sigma_\tau \sigma_\omega)$, and using the fact that the longitudinal coherence length for an electromagnetic mode with frequency content σ_ω is $\sigma_{lc} = 1/(2\sigma_\omega)$** we can write:

$$\delta^2 = \sigma_{lc}/\sigma_\tau = 1/M \qquad (2)$$

where M is the number of modes contained in the bunch. Equation (2) leads to the nice physical interpretation that the intensity fluctuation is due to M independent modes radiating randomly within the bunch. In fact, the radiation from a single mode is a stochastic Poisson process whose intensity shows 100% fluctuation. When M of such modes radiate in a combined but independent way the resulting fluctuation scales as described by Eq. (2).

The results presented so far assumed a bunch with no transverse size. By including the effect of the finite transverse size for the example case of Gaussian transverse distributions one obtains:

$$\delta^2 = \left(1 + \sigma_\tau^2/\sigma_{lc}^2\right)^{-\frac{1}{2}} \left(1 + \sigma_x^2/\sigma_{xc}^2\right)^{-\frac{1}{2}} \left(1 + \sigma_y^2/\sigma_{yc}^2\right)^{-\frac{1}{2}} \qquad (3)$$

with σ_x and σ_y the rms horizontal and vertical beam sizes respectively and σ_{xc} and σ_{yc} the coherence sizes of the related transverse electromagnetic modes at the wavelength of operation. Such quantities are defined by the properties of the radiation process and include diffraction effects due to limiting apertures. For simple cases analytical expressions for σ_{xc} and σ_{yc} can be derived and for more complex cases codes as SRW [7] can to be used.

It can be shown that the statistical error on δ^2 when N_s samples are collected is given by:

$$\sigma_{\delta^2}/\delta^2 = \sqrt{2/N_s} \qquad (4)$$

We tested the described theory with the ALS beam and the results were compared with the ones from streak camera measurements. Figure 2, shows the layout of the experimental setup used for the measurements performed at the beamline BL7.2. Such a beamline collects the synchrotron radiation from a dipole magnet and has a total angular acceptance of 5.5 mrad and 2.8 mrad for the horizontal and vertical plane respectively (represented by the limiting aperture in Fig. 2). BL7.2 spectrum ranges from the far-infrared up to the top part of the visible portion.

In our application we used visible light, which is in the incoherent part of the spectrum and allows using the large

** For a Gaussian pulse the uncertainty principle requires $\sigma_\tau \cdot \sigma_\omega = 1/2$.

variety and relatively inexpensive optical components and detectors readily available for such a frequency range. A 1 m focal length lens was used to focus through a flat mirror the beam on the photocathode plane of a streak camera (Hamamatsu C5680). The mirror could be retracted in order to allow for the light to go into another branch for the fluctuation measurement. An interferometric filter (Melles Griot), with gaussian transmission curve centered at 632.8 nm and with peak transmission of 55%, selected the photons within a bandwidth of 1 nm FWHM. The first lens focal length was chosen for keeping the angle between the incoming photon trajectories and the normal to the filter plane small enough to avoid broadening of the filter bandwidth. Downstream of the filter the transmitted photons were finally focused by a microscope objective (Edmund DIN 10, F 0.25) on the 0.2 mm^2 sensitive area of an avalanche photodiode (Perkin Elmer C30902S, gain 250, ~600 MHz bandwidth, ~ 60% quantum efficiency at 632.8 nm). The signal from the photodiode was amplified (Hamamatsu C5594, 50k-1.5G Hz bandwidth, 36 dB gain) and sent to a digital oscilloscope (LeCroy Wavepro 7300 A, 3 GHz bandwidth and 20 Gsamples/sec) for data recording and analysis. The oscilloscope was triggered with the ~ 1.5 MHz revolution clock of the ALS.

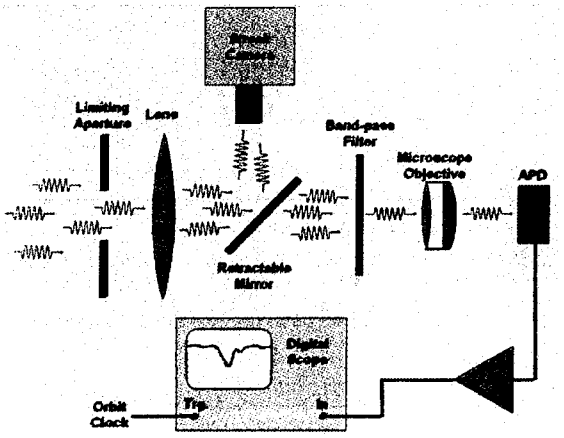

Figure 2. Schematic diagram of the experimental set-up used for the measurement at BL 7.2.

Figure 3, shows the typical signal visible at the scope when measuring the light from a single passage of a single ALS bunch. The typical rms length of the electron beam is ~ 25 ps so that the shape of the pulse in Fig. 3 was totally defined by the response of the measurement system. The oscilloscope was set in order to measure the areas S_{AB} of the signal between points A and B, and S_{CD} between points C and D in Fig. 4. S_{AB} is proportional to the number of photons impinging on the detector plus the contribution due to the noise in the signal, while S_{CD} is a measure of this noise contribution. The "lengths" of the segments AB and CD were set to be the same.

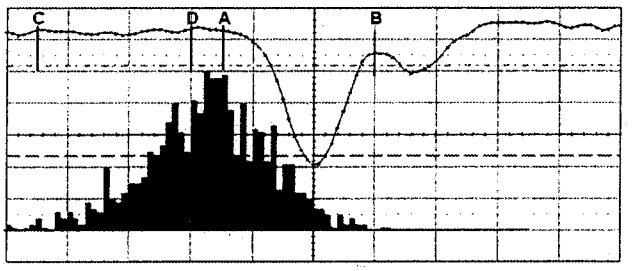

Figure 3. Oscilloscope window showing the track of a typical signal from the photodetector and the histogram of the measured values of the signal area between points A and B. The horizontal scale is 500 ps/div while the vertical is 50 mV/div.

The scope was also set to calculate the average values for such areas and their standard deviations over 5000 samples per each bunch length measurement (~ 1 min per measurement) in order to keep according to (4), the statistical error at ~ 2%. In this configuration, $\langle W \rangle$ the average energy radiated per passage by the electron beam is proportional to $\langle S_{AB} \rangle - \langle S_{CD} \rangle$, while its variance σ_W^2 is proportional to $\sigma_{SAB}^2 - \sigma_{SCD}^2$. By comparing different amplitude signals, we also verified that the shape of the signal itself did not depend on the amplitude.

Simulations and analytical calculations showed that in our configuration, the diffraction due to the finite beamline acceptance fully defines the shape for both the transverse modes, which can be well described by the $[\sin(\xi)/\xi]^2$ function typical of a plane wave diffracting through a finite aperture. Nevertheless, calculations also showed that it is still possible to use the Gaussian formula (3) if one fits the central peak of the $[\sin(\xi)/\xi]^2$ function with a gaussian, and uses for the coherence length the rms width of the fit divided by the $\sqrt{2}$ factor. For $\lambda = 632.8$ nm and for the acceptances of BL7.2 we obtained $\sigma_{xc} = 29.8$ μm and $\sigma_{yc} = 59.5$ μm. The ALS measurements were performed at the two beam energies of 1.2 and 1.9 GeV. The rms beam sizes at BL7.2 source point are $\sigma_x = 64.8$ μm and $\sigma_y = 6.3$ μm at 1.2 GeV and $\sigma_x = 103.0$ μm and $\sigma_y = 10.0$ μm at 1.9 GeV.

Equation (3) was derived in the framework of classical field theory, the proper quantum treatment requires the addition of the shot noise term $1/\langle N \rangle$, with $\langle N \rangle$ the average number of photons impinging on the detector. Additionally, photodiodes, avalanche photodiodes and photomultipliers all exploit stochastic phenomena for the photon-electron conversion and amplification. This must be accounted by using a modified shot noise term $\kappa^2/\langle N \rangle = \zeta/(\eta \langle N \rangle)$, where ζ is the excess noise factor, a constant ≥ 1 related to the avalanche process and η is the detector quantum efficiency. Putting all the contributions together and

indicating with $\delta_M{}^2$ the measured fluctuation variance one finally obtains for the rms length of the bunch:

$$\sigma_\tau^2 = \frac{1}{4\sigma_\omega^2}\left[\left(\delta_M^2 - \frac{\kappa^2}{\langle N\rangle}\right)^{-2}\left(1+\frac{\sigma_x^2}{\sigma_{xc}^2}\right)^{-1}\left(1+\frac{\sigma_y^2}{\sigma_{yc}^2}\right)^{-1} - 1\right] \quad (5)$$

The κ^2 term can be measured by performing 2 or more measurements of $\delta_M{}^2$ for the same bunch length for different number of photons impinging on the detector (using neutral density filters for instance). All the terms on both sides of (5) remain the same with the exception of the shot noise one. From that, and considering that $< N > \propto (< S_{AB} > - < S_{CD} >)$, κ^2 can be evaluated.

Figure 4 shows two examples of measurements performed for different beam conditions. The agreement with streak-camera data acquired right after each fluctuation measurement is remarkably good especially considering that no parameter has been adjusted to match the data.

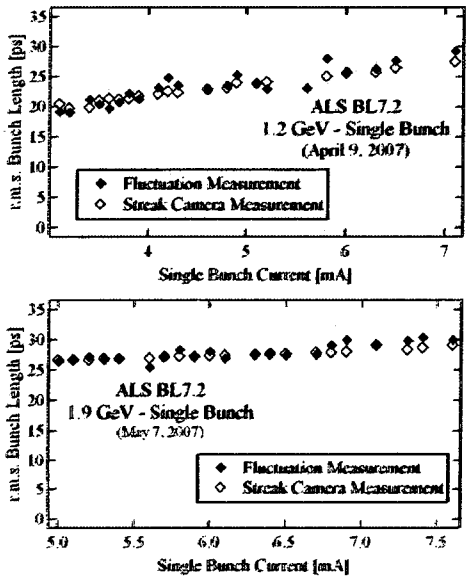

Figure 4. Examples of fluctuation and streak-camera bunch length measurements at the ALS for different beam parameters.

The typical rms difference between the streak camera and the fluctuation data was ~ 4 %. This is larger than the 2% contribution due to (4). The extra error is probably associated with the shot noise term that in our measurements was comparable to δ^2 and to the nonzero experimental error in the streak camera measurements.

Equation (3) and (5) show the dependency of the fluctuations on the transverse beam size. This situation can represent a limitation when the transverse beam size is not known a priori or when it varies shot to shot or turn to turn. In this case, by splitting the light from the source in two paths and using for each of them a bandpass filter with different central wavelength but same bandwidth, it is in principle possible to discriminate between the transverse and longitudinal components. This can be done by exploiting the fact that the longitudinal term depends only on the bandwidth of the filters while the transverse ones depend only on their central wavelength. By combining the results between the two branches it is then possible to remove the dependence of the measurement on the transverse size and measure the bunch length also in cases where the transverse beam size changes or is not known. This modified scheme is presently under test at the ALS.

We are also planning to test the system by coupling the light from the source to the measurement setup by an optical fibber. This will allow having the monitor components separated from the source area for an easy accessibility and tuning of the system.

A technique based on [3, 4] has been also successfully tested for measuring the length of the x-ray pulses in random emission processes [8, 9].

Pseudo-single bunch.

ALS as well as other light sources, dedicates several weeks per year to a mode of operation where two high current bunches are stored into diametrically opposed buckets. This special mode allows users to perform experiments requiring a long relaxation time. The photons from the main bunches excite their samples and the gap between the two bunches (~ 330 ns) permits data taking during the sample relaxation without the contaminating radiation from other bunches. During standard multibunch operation at the ALS ~ 280 contiguous buckets of the 328 available are filled with electrons. A single high current bunch (the "camshaft") is then injected in the remaining ~100 ns gap of empty buckets. Unfortunately, for most of the long relaxation time experiments, the empty bucket gap is too small for them to take data.

Table 3: Fast kicker system characteristics

Parameter	**Value**
Kicker type	Stripline
Electrode length	0.6 m
Characteristic impedance	50 Ohm
Deflection angle	73 μrad/kV
Pulse amplitude	1 kV
Repetition rate	~ 3 MHz (max)
Kicker Pulse width	~ 60 ns FWHM
Shot to shot stability	< 2.5 x 10^{-3}

To overcome this problem and to allow data taking for these experiments during standard multibunch operation, a new scheme of operation has been developed and is under test at the ALS.

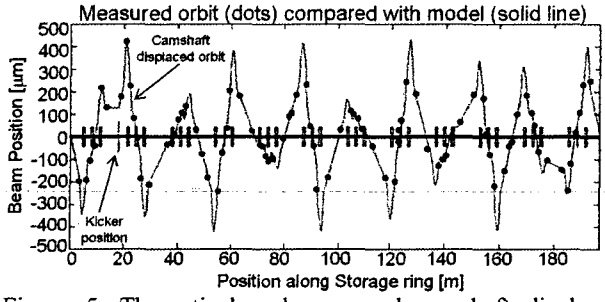

Figure 5. Theoretical and measured camshaft displaced orbit.

A fast kicker system capable of selectively kicking turn by turn the camshaft without perturbing the other bunches in the ring was constructed and installed in the ALS ring. Table 3 shows the main parameters of the system. By using such a kicker to synchronously kick the camshaft, one can force it on a stable vertically displaced orbit. The users in the beamlines where the displacement is large enough, can collimate out the photons from the other bunches and take the radiation only from the displaced camshaft, and operate in this way in a pseudo-single bunch mode parasitically to the standard multibunch operation.

Figure 5 shows the remarkable agreement between the theoretical displaced camshaft orbit (solid line) and the actual orbit (dots) measured when the kicker was operated at 1.522 MHz (ALS revolution frequency) with a ~750 V excitation (~ 55 μrad kick). The figure also shows how in some of the beamlines (position along the ring) the displacement is large enough to allow them to operate in the pseudo-single bunch mode.

By kicking the bunch every n-th turn instead of every turn, distorted orbits closing in n-turns can be generated. In this way, one can control the "repetition rate" of the pseudo single bunch and also create the required displacement in all beamlines.

The displacement amplitude can be controlled by exploiting the fact that the orbit is proportional to $1/\sin(\pi\nu)$. By means of small changes in the vertical tune ν, one can tune the displacement to the desired amplitude.

Local single bunch-closed bumps can be also obtained if more than one kicker is used.

Initial tests of the system at the ALS have been very encouraging and promising but before the pseudo-single bunch can become an official mode of operation, extensive further tests need to be done. For example, the transparency of the operation for the all the "normal" beamlines not using the pseudo-single bunch must be systematically and carefully investigated. More detailed information on the system can be found elsewhere [10].

FPGA based "bunch cleaning".

In the previous section, we described the special mode of operation of the ALS where two high current bunches are stored in the ring for allowing experiments requiring a long relaxation time. During this time, the gap between the two bunches must be free of electrons to avoid data contamination from photons radiated by undesired electrons stored in these nominally empty buckets. Unfortunately at the ALS and in other rings as well, because of imperfect injection, some of the "empty" buckets can be populated with electrons at a level of the order of 0.1% respect to the number of particles in the main bunches. Additionally as time flows, diffusion effects can progressively populate originally empty buckets. These contamination mechanisms can represent a severe limitation for a number of users that require bunch "purity" of 10^{-4} or better. For those users a bunch cleaning technique capable of removing the undesired particles is then required.

The cleaning system we presently use at the ALS is based on the scheme in operation at the Spring 8 storage ring [11] and tested at the ESRF [12]. The system layout is shown in Fig. 6, two signals are mixed together, amplified and sent to a transverse kicker that applies the excitation to the beam. One of the signals is a sinusoidal excitation at the frequency of one of the transverse tune sidebands, while the other is a pseudo-square wave synchronous with the ring RF and with zero amplitude crossing at the position of each of the bunches that needs to be preserved. After the mixing, the resulting signal is still a resonant excitation at the selected tune frequency but with zero amplitude at the position where "good" buckets are located. Such a signal, properly amplified and applied to the beam through the kicker, allows for the removal of the electrons in the undesired bunches by exciting them on very large transverse oscillations ending on the vacuum chamber walls.

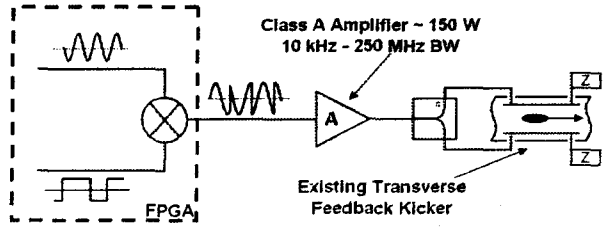

Figure 6. Bunch cleaning system layout.

Differently to the Spring 8 case, in the ALS implementation, the generation of both the signals and their mixing are performed digitally by using a low cost Xilinx demo-board (HW-V4-ML403-USA) with a 4VFX12 Virtex-

4 FPGA clocked at the ALS 500 MHz RF. The board also includes a DAC for the generation of the analogical output signal, and an imbedded Power-PC that allows network control of all the settings and functionality of the system.

At the ALS the bunch cleaning is performed in the storage ring right after injection, exciting the beam at one of the vertical tune sidebands. The sinusoidal frequency is actually swept over a bandwidth of 4 kHz to account for tune shift on amplitude effects. The kicker, a stripline with a transverse shunt impedance of ~ 9 kΩ, is one of the transverse feedback kickers. Despite this fact, the cleaning procedure is fully compatible with the transverse feedback operation (the high current bunches are not excited by the cleaning system) and no use of scrapers is required during the cleaning operation.

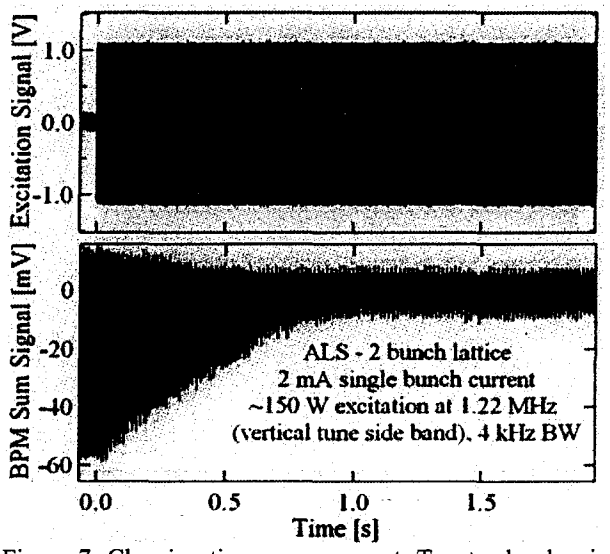

Figure 7. Cleaning time measurement. Top track: cleaning signal amplitude. Bottom track: sum signal from a beam position monitor.

The system has been extensively tested and has been regularly used in operation during the last few years. It showed a remarkable stability making the cleaning procedure straightforward and reliable. The perturbation on the good bunches during the cleaning is extremely small and even if the cleaning is presently performed with the shutters closed, there is the concrete possibility of doing it during users' data taking in a completely transparent way.

Figure 7, shows a measurement of the time required for the system for performing the cleaning. The top track is the excitation signal amplitude (switched ON for t=0) while the bottom track is the sum signal from a beam position monitor. From this measurement, one can estimate a time constant for the cleaning of ~ 0.4 s. It must be remarked that during this measurement the system was not fully optimised so significantly shorter time constants should be potentially achievable. The level of purity after a cleaning cycle is better than ~ 10^{-6}, beyond the measurement capability of our bunch purity monitor.

More detailed information on the system can be found elsewhere [13].

CONCLUSIONS

Despite being the oldest 3rd generation synchrotron light source in the world, ALS is still delivering quality beam with characteristics that compare well with the ones of the more recent storage ring based light sources. This is due to the continuous upgrade of the storage ring, of the beamlines and of the instrumentation and beam diagnostic systems that allow to control and tune the ALS to its maximum performance.

ACKNOWLEDGEMENTS

The authors acknowledge contributions from J. Byrd, S. De Santis, J. Guo, M. Hertlein, J. Kirz, D. Li, K. Robinson, R. Schoenlein, C. Steier, A. Trensim.

REFERENCES

[1] A. Jackson, *et al.*, Proceedings of 1994 European Particle Accelerator Conference, London, England, June 1994, pag. 107.

[2] H. Nishimura, *et al.*, Proceedings of 2007 Particle Accelerator Conference, Albuquerque, New Mexico, USA, 1997 pag. 1170.

[3] M. Zolotorev, G. Stupakov, SLAC PUB 7132 (1996).

[4] M. Zolotorev, G. Stupakov, Proceedings of the 1997 Particle Accelerator Conference, Vancouver, B.C., Canada, May 1997, pag. 2180.

[5] P. Catravas *et al.*, Phys. Rev. Letters **82**, 5261, (1999).

[6] V. Sajaev, *Determination of Longitudinal Bunch Profile using Spectral Fluctuations of Incoherent Radiation*, Proceedings of EPAC 2000, Vienna.

[7] SRW code, http://www.esrf.eu/Accelerators/Groups/InsertionDevices/Software/SRW

[8] E. Saldin, *et al.*, Opt. Commun. **148**, 383 (1998).

[9] M. Yabashi, *et al.*, Phys. Rev. Letters **97**, 084802 (2006).

[10] G. Portmann, *et al.*, this conference.

[11] H. Suzuki, *et al.*, Nuclear Instruments and Methods in Physics Research A **444** (2000) 515-533.

[12] E. Plouviez, ESRF Machine Technical Note 01-04/MDT.

[13] M. Chin, *et al.*, this conference.